Fabrication of a novel nano phase change material emulsion with low supercooling and enhanced thermal conductivity

Guanhua Zhang[1*], Zhenjie Yu[1], Guomin Cui[1], Binlin Dou[1], Wei Lu[1], Xiaoyu Yan[2]

[1] School of Energy and Power Engineering, University of Shanghai for Science and Technology, Shanghai, 200093, China

[2] Environment and Sustainability Institute, University of Exeter, Penryn, Cornwall, TR10 9FE, UK

[*]Corresponding author. E-mail address: guanhuazhang@usst.edu.cn

Abstract

A novel nano phase change material emulsion (NPCE) with low supercooling and high thermal conductivity was prepared by sonication method. *N*-octadecane was employed as phase change material, multi-walled carbon nanotubes (MWCNTs) were utilised as high thermal conductivity material, and octadecanol was utilised as nucleating agent. The characterization and thermal properties of the nanoemulsions prepared with various concentrations of MWCNTs and octadecanol were measured and analysed by scanning electron microscopy (SEM), transmission electron microscopy (TEM), particle size analyzer, differential scanning calorimeter (DSC) and thermal conductivity meter. The results indicated that the nanoemulsions prepared had great stability, low supercooling and enhanced thermal conductivity. The thermal conductivity was enhanced by 4.32 % for 10 wt% nanoemulsion with addition of 1 wt% MWCNTs. The supercooling degree of 20 wt% nanoemulsion was decreased by 36.4 % from 17.3 ℃ to 11.0 ℃ with addition of 1 wt% octadecanol. It can be concluded that the nanoemulsions prepared were able to be utilised as heat transfer and energy storage fluids, with great potential in thermal system applications.

Keywords: Nanoemulsion; Phase change materials; Supercooling; Characterization; Thermal properties

Nomenclature	
ΔH_c	heat of crystallization (kJ/kg)
ΔH_f	heat of fusion (kJ/kg)
k	thermal conductivity (W/(m ^oC))
T	temperature (^oC)
T_m	melting temperature (^oC)
T_c	crystallizing temperature (^oC)
ΔT	supercooling degree (^oC)

1. Introduction

Thermal energy storage (TES) has great energy-saving potential and can reduce environmental pollution [1]. Latent heat storage using phase change material (PCM) to absorb latent heat during melting process and release latent heat during crystallization process is considered to be the most effective method for cold energy storage or heat recovery [2]. In the same temperature range, latent heat storage system has more energy storage capacity than sensible heat storage system. The high energy storage density also makes the volume of the latent heat storage system smaller and is the reason for its constant temperature characteristics [3]. Latent heat storage absorbs and releases heat within a very small range of or at a specific temperature during phase transition [4]. PCM can be classified into four categories and solid-liquid PCM are the most common materials that have been extensively investigated due to their easily controllable volumes [5]. Microencapsulated phase change material slurry and phase change material emulsions presented great potential in air-conditioning systems and solar thermal systems [6-8]. Intensive investigations have been carried out by numerous researchers on the fabrication, flow, heat transfer characteristics and thermal properties of microencapsulated phase change material slurry and phase change material emulsions.

Microencapsulated phase change material slurry has some disadvantages such as complex preparation process, risk of microcapsule leakage, ease of demulsification during usage and long-term slurry instability. Alkan and Sari [9] prepared four kinds of fatty acid/poly methyl methacrylate microcapsules and the results indicated that form-stable fatty acid/PMMA microcapsules had great prospect in the industrial applications of latent heat thermal energy storage. Liu et al.[10] prepared phase change microcapsules with lauryl alcohol as PCM and melamine-formaldehyde inclusion graphite as shell by in-situ polycondensation. It was found that the phase change temperature of microcapsules was close to that of pure paraffin while the specific heat and thermal conductivity of microcapsules were higher than that of pure paraffin.

Investigation were also carried out on the addition of tetradecanol as nucleating agent into *n*-tetradecane microcapsules was conducted by Alvarado et al. [11]. The results showed that the addition of 2 % or 4 % *n*-tetradecanol had a great inhibitory effect on supercooling. Zhu et al. [12] respectively used *n*-dodecane (C12) and *n*-tetradecane (C14) as PCM to synthesis microcapsules by in-situ polymerization. A small amount of *n*-hexatriacontane (C36) was added to the microcapsule as nucleating agent. When the mass fraction of C36 was 3wt %, supercooling of C12 and C14 microcapsules was reduced to 5.8 ^{o}C and 2.9 ^{o}C, respectively. Al-shannaqetet al. [13] selected RT58 and 1-octadecanol as nucleating agents to reduce or eliminate supercooling in the microcapsules. The onset crystallization temperature of RT21 phase change microcapsules shifted from 10.9 to 19.8 °C when 5wt% of RT58 was added. The addition of 1-octadecanol had a negative effect that made the temperature range of crystallization process wider. Ahmet et al. [14] synthesized a series of polystyrene(PS)/(tetracosane(C24)–octadecane(C18)) micro/nano phase change capsules by using emulsion polymerization method, the results show that the micro/nanocapsules prepared can be utilised for low-temperature latent heat thermal energy storage. Furthermore, Wang et al.[15] prepared a novel microencapsulated PCM which showed great potential for solar energy storage and intelligent textiles.

Phase change emulsion has advantages such as simple preparation process, good stability and low cost. In recent years, many researchers have investigated properties of phase change emulsion and its application in the engineering field. Two novel solid-liquid phase change fluids, phase change microcapsule slurry and phase change material emulsion have been proposed [16]. Mo et al.[17] added L-MWNT-1030, L-MWNT4060 and L-MWNT-60100 into deionized water to prepare nanofluids. The mass fraction of surfactants and the size of carbon nanotubes varied with supercooling and freezing time. The supercooling degree and the initial solidification time of nanofluids prepared using L-MWNT-1030 were lower than those of deionized water. The nucleation mechanism and stability of nanofluids also affected the solidification behaviour of the solution. Liu et al. [18] investigated supercooling and nucleation rate of nanofluids prepared by deionized water and graphene as additive particle. The results show that the supercooling degree of deionized water was 31.5 K. The supercooling degree of the nanofluids with various concentrations of graphene was 7.98, 7.93, 3.05 and 3.03 K, respectively, which indicated that the supercooling degree decreased by more than 74 % with increase in graphene.

Huang et al. [19] showed that different surfactants had no effect on the supercooling while nucleating agents had an effect on the melt and solidification temperature of the emulsion, which could effectively reduce the supercooling degree. Shao et al.[20] indicated that supercooling, stability and viscosity of phase change emulsions are related to each other and a balance among them was needed. Wang et al. [21] prepared 30 % paraffin emulsion with 2.0 % nano-graphite and the supercooling degree was reduced from 9.9 ℃ to 0 ℃, and the viscosity was lower than that of 11.5 mPa·s. Zhang et al. [22] developed a phase change emulsion with *n*-hexadecane and modified CNTs as nucleating agent. The result showed that the supercooling degree of the emulsion was reduced by 43 %. Shao et al. [23] developed a novel paraffin-water emulsion with RT10. The heat storage capacity of emulsion was almost twice as much as that of water and its supercooling was reduced to 0.2℃. Nevertheless, the viscosity of the emulsion was much higher than water while the value of thermal conductivity was

lower.

Zhang et al. [24] added 0.1 wt% MWCNTs as nucleating agent into *n*-hexadecane/water emulsion and the supercooling degree of emulsion was decreased by 3.68 ℃. In addition, they modified the surface of MWCNTs. When the concentration of the modified MWCNTs was 0.6 wt%, the supercooling of emulsion was reduced by 14.67 ℃. The emulsion of a lower viscosity was prepared by Wang et al. [25] with paraffin wax as PCM and polyvinyl alcohol (PVA), polyethylene glycol (PEG 600) and 0.05 % nano-graphite as dispersants. The heat storage density of the emulsion was twice that of water. Several nano-fluids were prepared by Salla et al. [26], the melting temperature of the emulsion was 3-4 ℃ lower than those of bulk materials. The latent heat value was basically consistent with the theoretical value, and the specific heat capacity of the emulsion was 3 % different from the theoretical value. Zhang et al. [27] prepared composite fatty acid emulsion using sebacic acid and lauric acid as PCM and the supercooling degree was reduced from 20 ℃ to 10 ℃ after adding hexadecanol as nucleating agent. Wang et al. [28] prepared polysiloxane capsules with erythritol as PCM by ultraviolet assisted hydrolysis. The thermal conductivity of polysiloxane capsules was 0.84 W/(m·K). The supercooling degree was reduced by 83.6 % and the exothermic ratio was increased by 52.2 % due to the improvement of crystallization kinetics.

There are two primary problems in the existing nano phase change material emulsion: low thermal conductivity and serious supercooling during the crystallization process. Supercooling occurs when PCM transits from liquid to solid and the liquid still does not crystallize below the freezing point [29]. Therefore, there will be a temperature interval at the time of charging and releasing, which affects the performance of the latent heat storage system. A lower supercooling degree and a higher thermal conductivity improves the energy efficiency of the system and the phase change process of PCMs [30]. However, there are limited studies in the literature to solve the above two problems simultaneously. Therefore, the aim of this paper was to propose a novel PCM nanoemulsion that can improve the thermal conductivity and effectively decrease the supercooling degree. This paper builds

on previous investigations [31, 32] and fabricated a series of PCM nanoemulsions with high thermal conductivity and low supercooling degree. In addition, the proposed fabrication method reduced fabrication cost of PCM nanoemulsion as the shell material was eliminated in the fabrication process.

2. Method and materials

2.1. Materials

N-octadecane (99 wt% purity), multi-walled carbon nanotubes (99 wt% purity), and octadecanol (99 wt% purity) were supplied by Macklin Inc, Shanghai. Sodium dodecyl sulphate (SDS) was provided by Sinopharm Chemical Reagent Co., Ltd, Shanghai.

2.2. Synthesis of PCM nanoemulsions

10 wt.% of *n*-octadecane and 20 wt.% of *n*-octadecane were chosen due to NPCEs made with 10 wt.% of *n*-octadecane and 20 wt.% of *n*-octadecane have appropriate viscosity for using as the heat transfer and energy storage fluids. Five kinds of NPCEs containing 10 wt% *n*-octadecane with different concentrations of MWCNTs (0 wt%, 0.1 wt%, 0.25 wt%, 0.5 wt%, and 1.0 wt%) were prepared. Secondly, three kinds of NPCEs with 10 wt% *n*-octadecane containing 0.1 wt% MWCNTs with various concentrations of octadecanol (0.25 wt%, 0.5 wt% and1.0 wt%) were prepared. As the viscosity of 20 wt% NPCE is high, the dispersing of 0.25 wt% in the NPCE is difficult. Therefore, only 20 wt% NPCE containing 0.1wt% MWCNTs with various concentrations of octadecanol (0 wt%, 0.25 wt%, 0.5 wt%, and 1.0 wt%) were prepared. Table 1 shows all the samples prepared.

For the synthesis of 10 wt% NPCEs with 0.1 wt% MWCNTs and 0.25 wt% octadecanol, the surfactant solution was prepared by adding 2 wt% SDS into deionized water and stirring by a magnetic agitator (MS7-H550-S, AB Scientific Co., Ltd) at 50 ^{o}C for 15 minutes. 0.1 wt% of MWCNTs was mixed with the solution and stirring continued for another 15 minutes. In another beaker, 0.25 wt% octadecanol was dissolved in 10 wt% *n*-octadecane at 50 °C. The solution was mixed into the first beaker and stirred for 10 minutes at 50 °C. Then the mixed solution was placed in the ultrasonic water

bath for 30 minutes. Finally, the mixed solution was sonicated with an ultrasonic processor (Type JY92-IIN, LNB Instrument, Shanghai) at 70 % amplitude for 30 minutes. Fig.1 shows detailed synthesis process of PCM nanoemulsions.

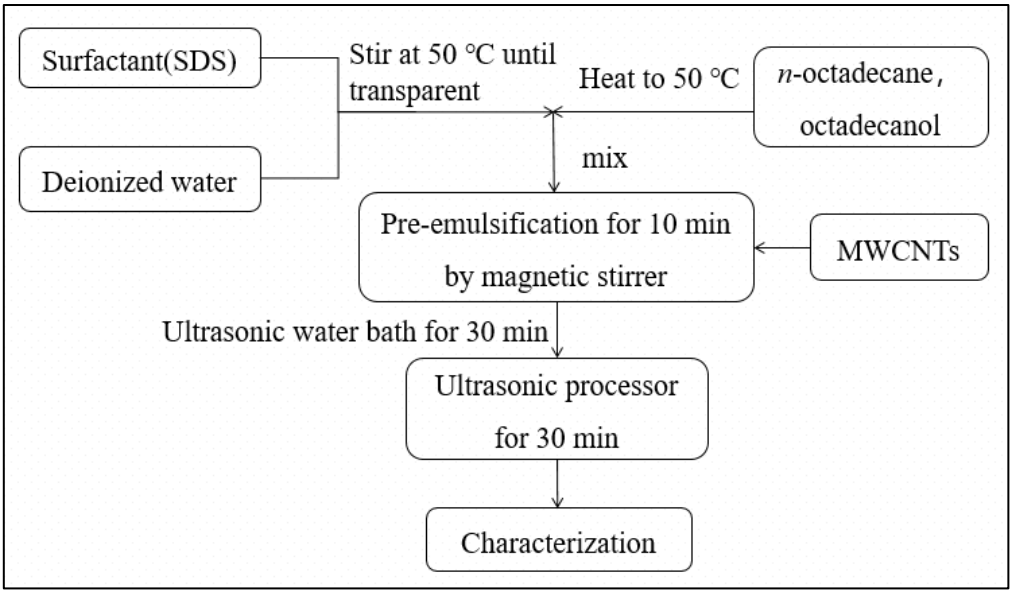

Fig.1. Schematic diagram of the synthesis process.

Table 1. Nanoemulsions prepared.

Sample	*n*-octadecane	SDS	MWCNTs	octadecanol	DI water
1	5g	0.5g	0g	0g	44.5g
2	5g	0.5g	0.05g	0g	44.45g
3	5g	0.5g	0.125g	0g	44.375g
4	5g	0.5g	0.25g	0g	44.25g
5	5g	0.5g	0.5g	0g	44g
6	5g	0.5g	0.05g	0.125g	44.325g
7	5g	0.5g	0.05g	0.25g	44.2g
8	5g	0.5g	0.05g	0.5g	43.95g
9	10g	1g	0g	0g	39g
10	10g	1g	0.05g	0g	38.95g
11	10g	1g	0.05g	0.125g	38.825g
12	10g	1g	0.05g	0.25g	38.7g
13	10g	1g	0.05g	0.5g	38.45g

2.3 Characterization of MWCNTs

The characterization experiments of MWCNTs were carried out using field emission environment scanning electron microscope（FESEM-Quanta FEG 450）and field emission transmission electron

165 microscope（HRTEM-Tecnai G2 F30）.

166 **2.4. Particle size analysis of PCM nanoemulsions**

167 Dynamic light scattering (DLS) technique was employed to measure the particle size distribution and
168 particle dispersion index (PDI) of NPCEs with a particle size analyser (Nano-Zeta sizer, Malvern
169 Instruments). The accuracy of the mean droplet size d50 is ±1 %. The NPCE was diluted with
170 deionised water at a proportion of 1:50 in a 20ml glass cuvette, and the measurement sensitivity is 0.1
171 mg/mL.

172 **2.5. Thermal properties of PCM nanoemulsions**

173 The thermal properties of NPCEs was determined using DSC (200F3 Maia, NETZSCH), and the DSC
174 was calibrated prior to tests. 10-20 mg of emulsion was prepared in an aluminium crucible. The
175 sample was measured at a heating/cooling rate of 2 K/min in nitrogen atmosphere. In order to ensure
176 the accuracy of the measurements, all samples were tested three times. The melting/crystallization
177 heat and melting/crystallization point can be obtained using the DSC analysis program and the DSC
178 test results were further analysed and mapped using OriginPro9.

179 The thermal conductivity of NPCEs was measured using thermal conductivity instrument (DZDR-S,
180 NANJING DAZHAN). The specified accuracy of the instrument is ±3 % depending on the sample
181 size, conductivity and reproducibility. The thermal conductivity of all samples was measured when
182 PCM was in solid and liquid states. Five measurements were taken for each sample and each
183 measurement had an interval of 5 minutes. The mean values of those measurements were employed.

184

185 **3. Results and discussion**

186 **3.1. Microstructure analysis of MWCNTs**

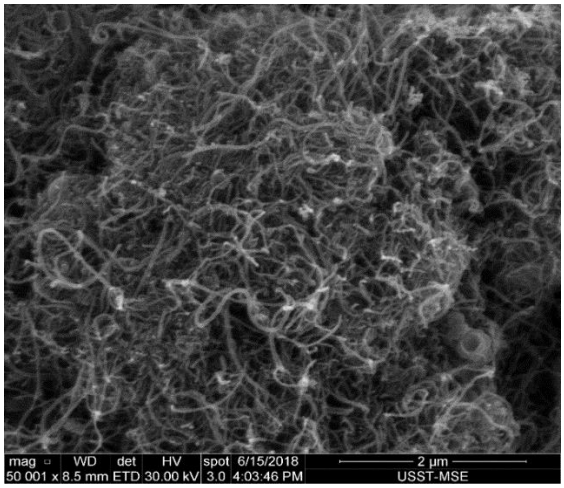

Fig.2. SEM image of MWCNTs.

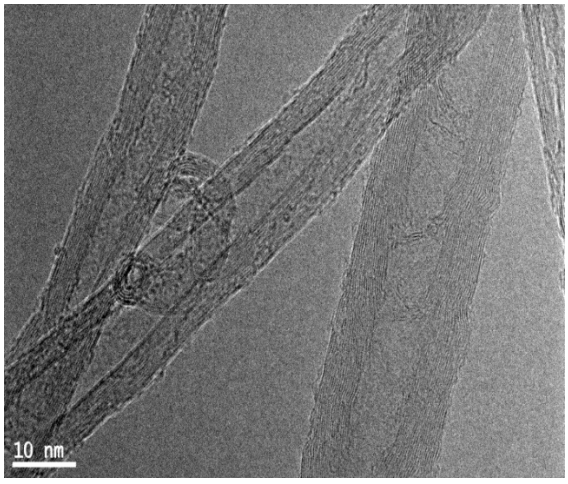

Fig.3. TEM image of MWCNTs.

Figure 2 and Figure 3 show SEM and TEM images of MWCNTs, respectively, where the internal structure of carbon nanotubes can be seen clearly. All carbon nanotubes have multi-layer walls with an inner diameter of about three nanometers. The outer diameter is about 10 nanometers. The intrinsic thermal conductivity of MWCNTs is as high as 3000 W/(M·K). Low density and high specific surface area make it the best choice to enhance the thermal properties of PCM in the application of weight and volume limitation. In addition, the thermal conductivity of MWCNTs is higher than that of some conventional materials [33].

3.2. Particle size analysis of NPCEs

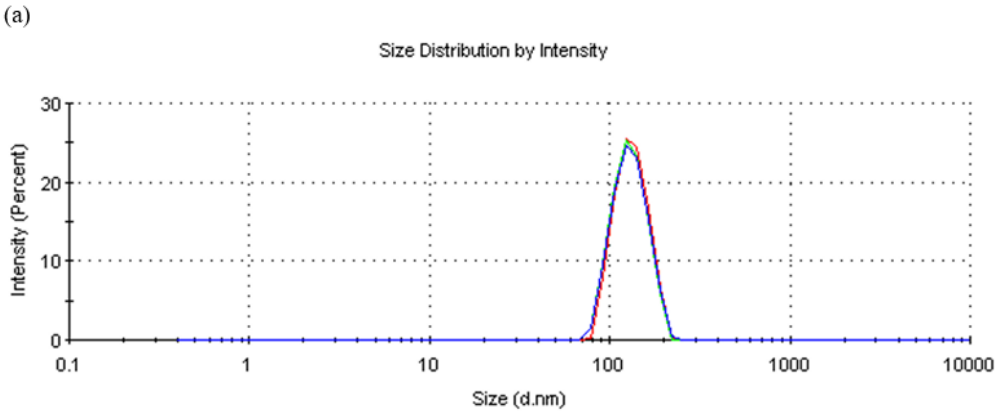

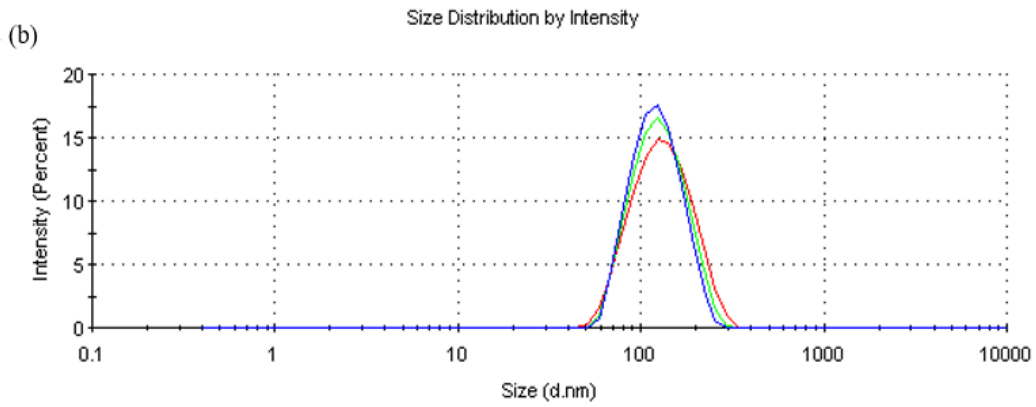

196

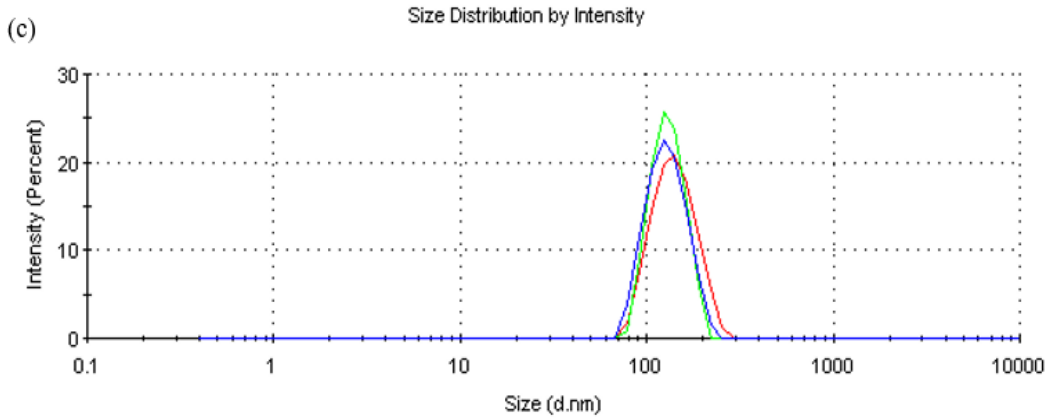

197

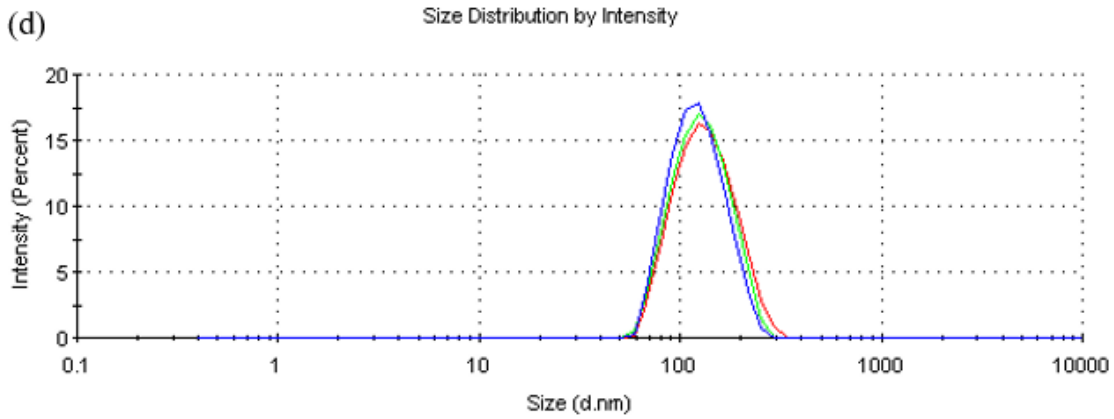

198

199 **Fig.4**. (a) Particle size distribution of 10 wt% NPCE, (b) Particle size distribution of 10 wt% NPCE
200 with 0.1 wt% MWCNTs, (c) Particle size distribution of 10 wt% NPCE after three month settlement,
201 and (d) Particle size distribution of 10 wt% NPCE with 0.1wt% MWCNTs after three month
202 settlement.

203 Figure 4 shows the particle size distribution of 10 wt% NPCE with 0.1 wt% MWCNTs and 10 wt%

NPCE without MWCNTs before and after three months. Three curves of different colours suggest that three measurements of the same sample are very close to each other. The particle size distribution of 10 wt% NPCE is between 70 nm and 220 nm as shown in Fig. 4(a). In addition, the results show that the average Z particle size of 10 wt% NPCE is 128.2 nm, and the average value of PDI is 0.010. Fig. 4(c) is a diagram of 10 wt% NPCE particle size after three-month settlement. The results show that its particle size distribution is between 78~255nm, the average Z particle size is 132.5 nm and the average value of PDI is 0.106. Fig. 4(b) shows the particle size of 10 wt% NPCE with 0.1wt% MWCNTs, which had just been prepared. The results suggest that the particle size distribution is between 50~255nm, the average Z particle size is 123.5 nm and the average value of PDI is 0.149. Fig. 4(d) displays the particle size of 10 wt% NPCE with 0.1 wt% MWCNTs after three-month settlement. The results suggest that the particle size distribution is between 58~255nm, the average Z particle size is 125.5 nm and the average value of PDI is 0.119. Therefore, these results demonstrated that the dispersion and stability of the emulsions were still excellent after three-month settlement and also proved that the ultrasonic water bath and ultrasonic sonication methods were effective in the experiment. A study by Asua et al. [34] showed that longer ultrasonic action time offered smaller particle size of emulsion. Compared with the emulsion prepared by ordinary stirring, the fine emulsion has very low polydispersity [35]. Therefore, the PDI index measured in this paper is of universal significance.

3.3. DSC analysis of NPCEs

Figure 5 shows the DSC curve of *n*-octadecane. The melting peak value is 30.9 ^{o}C and the crystallization peak value is 24.2 ^{o}C. Fig. 6 shows the DSC curves of 10 wt% *n*-octadecane with different concentrations of MWCNTs. All samples have similar shapes but different areas. All the samples display obvious supercooling phenomenon, and the crystallization temperature is about 14 ~ 16 ^{o}C below the melting temperature. The supercooling degree of 10 wt% *n*-octadecane emulsion is 14.86 ^{o}C. From the melting curve, two peaks appear gradually with the increase in CNT concentration.

When CNT is 1.0 wt%, the height of the right peak exceeds the left peak, and the supercooling degree of emulsion reaches 17.8 °C. This may be due to the simultaneous ultrasonic fragmentation of CNT and PCM. With the increase in CNT concentration, a larger part of the oil in water droplets is encapsulated with CNT particles, thereby changing the melting behaviour of the emulsion and resulting in two melting peaks. Eva et al. [36] also pointed out that the enthalpy of phase transition and melting temperature were also affected by the shape of PCM droplet. The melting peak temperature of the *n*-octadecane emulsion prepared is between 26 °C and 27 °C. The possible reasons are as follows: first, the emulsion with large specific surface area leads to the premelting of a large percentage of PCM; and second, the droplet size decreases the melting enthalpy. When the surfactant is dissolved in PCM, the melting temperature of PCM and the enthalpy of phase transition are decreased. This may be considered a side effect of emulsification [36].

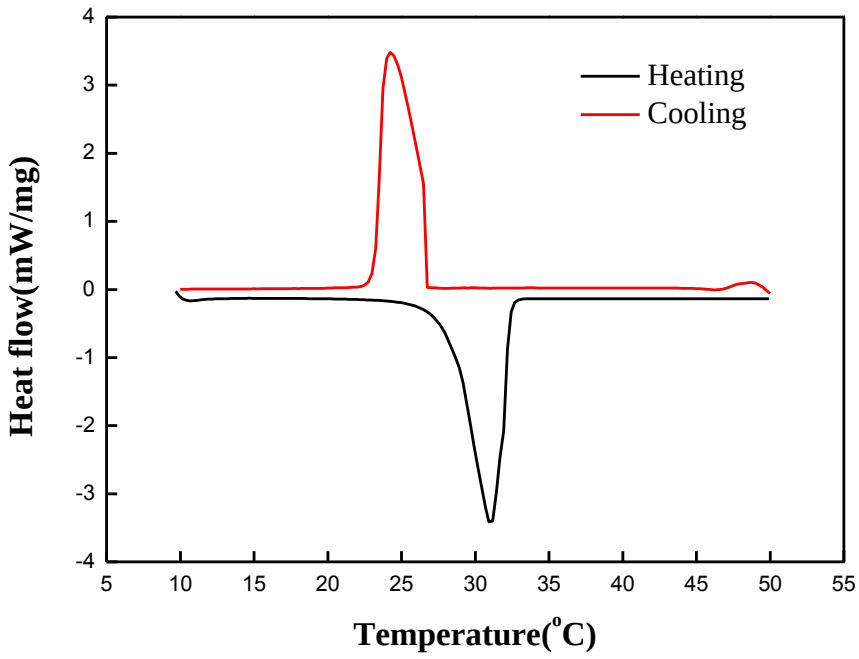

Fig.5. DSC curve of pure *n*-octadecane.

There are two peaks in the crystallization curve in Fig. 6, and the solidification temperature of all emulsified samples reduced dramatically. Firstly, the heat transfer theory can be used to explain that when the local temperature reaches nucleation temperature, the first particle solidified and released

the latent heat, dispersing the heat into the emulsion and thereby inhibiting the nucleation of nearby particles. The next particle solidifies when the heat releases from the first particle solidifies. Secondly, the crystallization process of pure alkane PCMs with constant nucleation temperature is due to homogeneous nucleation or heterogeneous nucleation. The supercooling of the emulsion, however, is related to unbalanced and inadequate heterogeneous nucleation, which usually occurs in solutions containing impurity particles [35]. This phenomenon can be explained by different seed types. For small droplets, the higher peaks in the curve are due to the nucleation or homogeneous nucleation of the droplet surface. The lower peak is due to further drop of droplet size, resulting in lower nucleation temperature [36]. In addition, the minor fluctuations in the melting processes may be caused by impurities in the emulsion or by impurities brought in by the preparation process of DSC test.

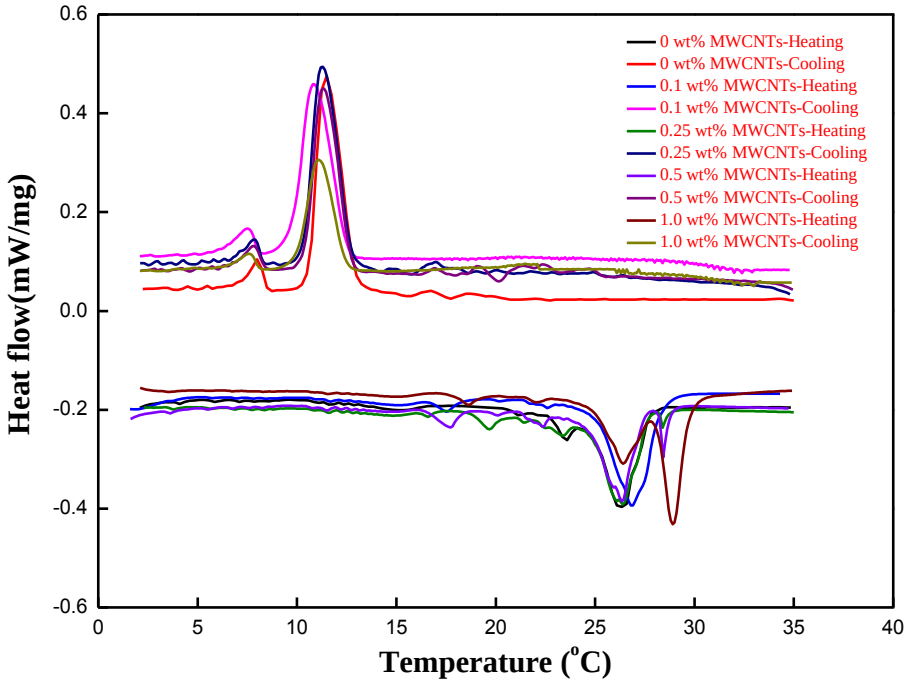

Fig.6. DSC curves of 10 wt% NPCE with various mass fractions of MWCNTs.

Table 2 summarizes the corresponding thermal properties of the six samples. Onset T_m, T_m and ΔH_f are defined as the initial phase transition temperature, peak temperature and latent heat value, respectively. Onset T_c, T_c and ΔH_c are defined as the initial phase transition temperature, peak temperature and latent heat value, respectively. The supercooling is the difference between the melting

peak temperature and the crystallizing peak temperature: $\Delta T = T_m - T_c$.

Table 2. Thermal properties of *n*-octadecane and 10 wt% NPCE with various mass ratios of MWCNTs.

Sample name	Onset T_m °C	Onset T_c °C	T_m °C	T_c °C	ΔH_f J/g	ΔH_c J/g	ΔT °C
N-octadecane	25.4	22.7	30.9	24.2	265.72	264.72	6.7
10wt% NPCE	25.2	10.4	26.4	11.5	18.68	22.87	14.9
10wt% NPCE+0.1wt% MWCNTs	24.7	10.0	26.9	10.9	17.35	21.77	16.0
10wt% NPCE+0.25wt% MWCNTs	25.0	10.5	26.4	11.3	16.34	21.06	15.1
10wt%NPCE+0.5wt% MWCNTs	24.8	10.5	26.3	11.3	17.04	22.20	15.0
10wt% NPCE+1.0wt% MWCNTs	28.5	10.3	28.9	11.1	19.18	12.31	17.8

Figure 7 shows the DSC curves of 10 wt% NPCEs containing 0.1 wt% MWCNTs with various concentrations of octadecanol (0 wt%, 0.25 wt%, 0.5 wt%, 1.0 wt%). First of all, there are two peaks in the crystallization curve. The left peak is lower and the position and area of the peak are almost unchanged with increase in octadecanol concentration. The area of the peak on the right is larger. With increasing octadecanol concentration, its position shifts further right, crystallization temperature becomes close to the melting temperature, and supercooling degree and area decreases gradually. In the melting curve, the melting peak temperature shifted to the right and the melting heat decreased with increase in octadecanol concentration.

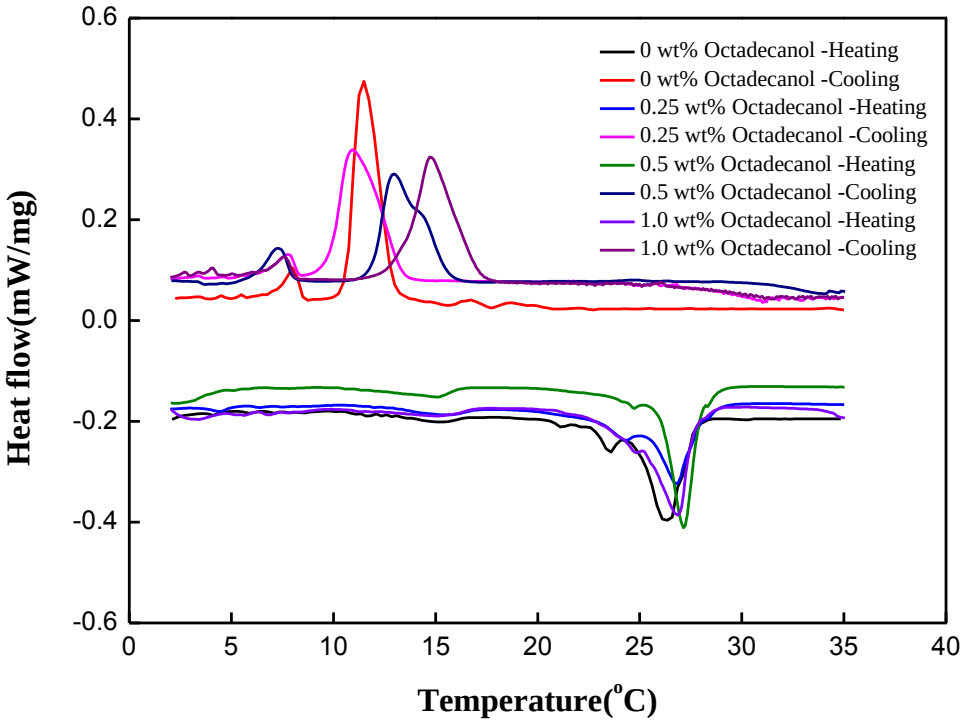

Fig.7. DSC curves of 10 wt% NPCE with 0.1 wt% MWCNTs and various mass fractions of octadecanol.

Figure 8 shows the DSC curves of 20 wt% NPCEs containing 0.1 wt% MWCNTs with various concentrations of octadecanol (0 wt%, 0.25 wt%, 0.5 wt%, 1.0 wt%). The curve is similar to that of 10 wt% *n*-octadecane emulsion, which further verifies the regularity of 10 wt% *n*-octadecane emulsion. As the *n*-octadecane concentration increases, the enthalpy values of melting heat and crystallizing heat increase about twice while the supercooling degree of the emulsion becomes lower than that of the *n*-octadecane emulsion with the same concentration of octadecanol. When 1.0 wt% octadecanol is added, the minimum degree of supercooling is 11 ℃. Table 3 summarizes the thermal properties of 10 wt% and 20 wt % nanoemulsions containing 0.1 wt% MWCNTs with various concentrations of octadecanol.

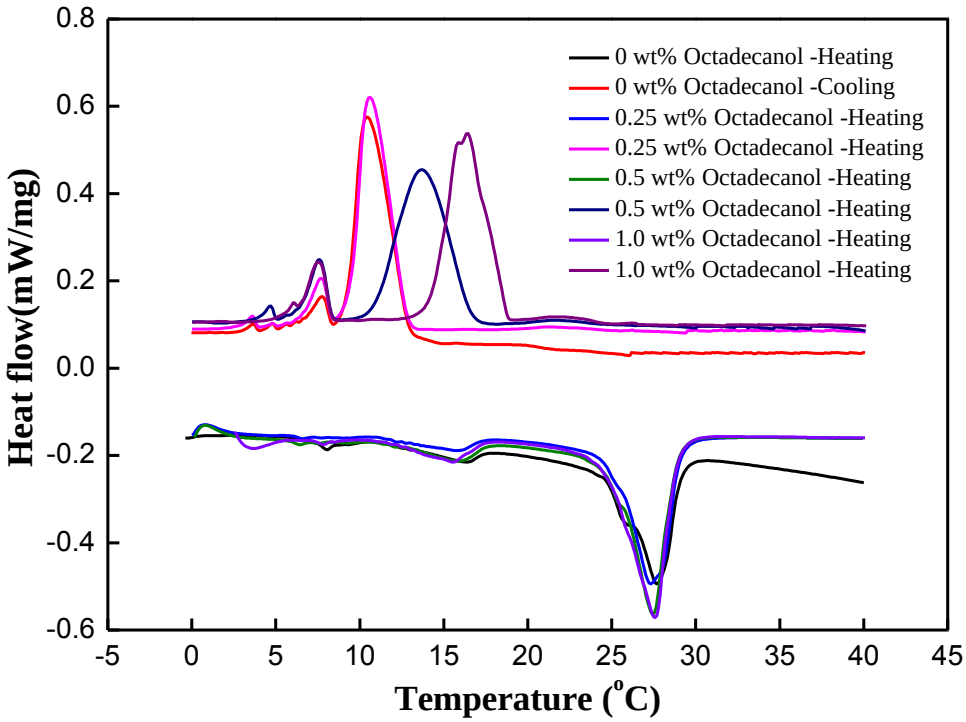

Fig.8. DSC curves of 20 wt% NPCE with 0.1 wt% MWCNTs and various mass fractions of octadecanol.

Table 3. Thermal properties of NPCEs (10 wt% and 20 wt%) with 0.1 wt% MWCNTs and various mass ratios of octadecanol.

Sample name	Onset T_m (ºC)	Onset T_c (°C)	T_m (°C)	T_c (°C)	ΔH_m (J/g)	ΔH_c (J/g)	ΔT (°C)
N-octadecane	25.4	22.7	30.9	24.2	265.72	264.72	6.7
10wt% NPCE+0.1wt% MWCNTs	24.7	10.0	26.9	10.9	17.35	21.77	16.0
10wt% NPCE+0.1wt% MWCNTs +0.25 wt% octadecanol	25.5	10.1	26.8	10.9	16.02	20.31	15.9
10wt% NPCE+0.1wt% MWCNTs +0.5wt% octadecanol	26.1	11.9	27.2	13.0	15.53	16.90	14.2
10wt% NPCE+0.1wt% MWCNTs +1.0wt% octadecanol	25.1	13.4	26.8	14.7	16.58	17.28	12.1
20wt% NPCE+0.1wt% MWCNTs	25.3	9.4	27.7	10.4	32.48	42.18	17.3
20wt% NPCE+0.1wt% MWCNTs +0.25wt% octadecanol	25.4	9.6	27.3	10.6	30.44	37.96	16.7
20wt% NPCE+0.1wt% MWCNTs +0.5wt% octadecanol	25.2	8.1	27.5	13.7	32.98	36.38	13.8
20wt% NPCE+0.1wt% MWCNTs +1.0wt% octadecanol	25.0	14.5	27.6	16.6	35.24	34.40	11.0

3.4. Thermal conductivity analysis of NPCEs

Figure 9a and 9b show the thermal conductivity and the corresponding reinforcement ratio of the mixed emulsion with various concentrations of MWCNTs for 10 wt% NPCE, respectively. The thermal conductivity was determined using thermal conductivity instrument. The thermal conductivity of 10 wt% *n*-octadecane nanoemulsion without MWCNTs is 0.5701W/(m·K) (solid state of PCMs) and 0.6176W/(m·K) (liquid state of PCMs). The thermal conductivity of nanoemulsion increases linearly with the increase in MWCNTs concentration. When the concentration of MWCNTs is 0.1 wt%, the thermal conductivities of nanoemulsion are 0.5751W/(m·K) (solid state of PCMs) and 0.6204W/(m·K) (liquid state of PCMs) and the corresponding enhancement ratios are 0.88 % and 0.45 %, respectively. When the concentration of MWCNTs reaches 1 wt%, the thermal conductivities of nanoemulsion reach the highest, which are 0.5923 W/(m·K) (solid state of PCMs) and 0.6443 W/(m·K) (liquid state of PCMs) and the corresponding enhancement ratios are 3.89 % and 4.32 %, respectively.

Grag et al. [37] indicated that the viscosity of the fluid decreases and the Brownian motion of the nanoparticles in the emulsion increases with increase in temperature, resulting in a convection effect that increases the thermal conductivity. In addition, the thermal conductivity of solid mixtures increases more under the same condition, which is due to the orderliness caused by directional crystallization [38]. However, for a liquid mixed solution, its thermal conductivity also increases, which is probably related to the arrangement of molecules, even in the liquid phase. The increase of thermal conductivity of liquid mixed solution is not obvious due to the randomness of liquid molecular orientation [39].

Xue et al. [40] showed that the effective thermal conductivity of composites increased rapidly with the increase in nanotubes length. However, the effective thermal conductivity varied little when the diameter of nanotubes exceeded one order of magnitude. In this paper, it is found that with the increase

in ultrasonic dispersion time, MWCNTs can be better dispersed in phase change emulsion, thus improving the thermal conductivity of emulsion. However, this may result in changing the length and diameter of MWCNTs, thus reducing the thermal conductivity of the emulsion. The balance between the two effects will be further investigated in future work.

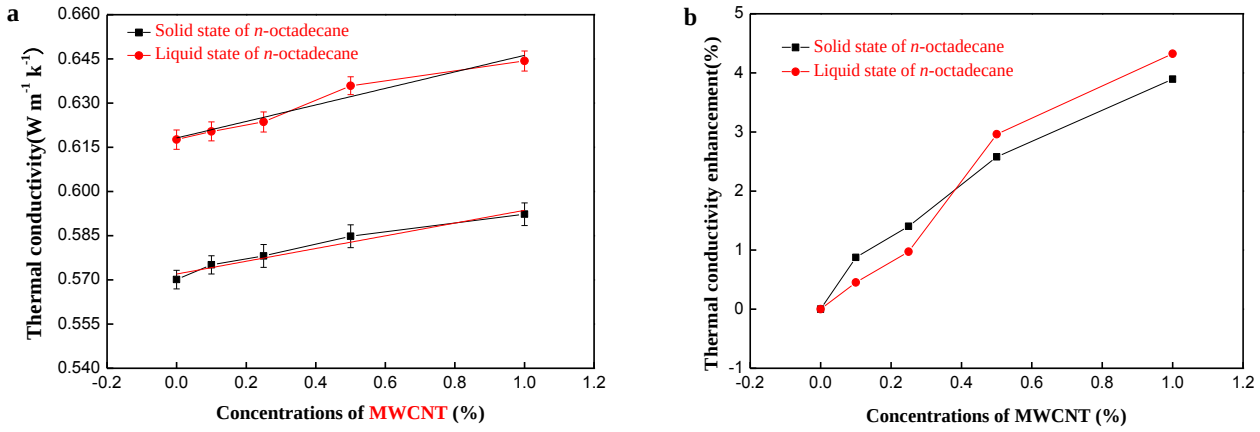

Fig.9. (a) Thermal conductivity of 10 wt% NPCE with various concentrations of MWCNTs, (b)Thermal conductivity enhancement of 10 wt% NPCE with various concentrations of MWCNTs.

Figure 10 shows the thermal conductivity of 10 wt% NPCE containing 0.1 wt% MWCNTs with various concentrations of octadecanol. It can be seen that with the increase in octadecanol concentration, the thermal conductivity of PCM in solid or liquid state decreases gradually, the thermal conductivity of water at 20 ℃ is 0.599W/(m·K), the thermal conductivity increases linearly between 0 ℃ and 100 ℃, while the thermal conductivity of octadecanol is 0.38 W/(m·K) at room temperature. Therefore, the decrease of thermal conductivity of nanoemulsion may be due to the decrease of water specific gravity with the increase in octadecanol concentration, which leads to the decrease of total thermal conductivity of nanoemulsion. When the concentration of octadecanol was 0.25 wt%, the supercooling decreased by 4.4 % and the thermal conductivity of nanoemulsion increased by 0.58 % (PCM at soild state) and 0.32 % (PCM at liquid state), respectively, compared with 10 wt% *n*-octadecane nanoemulsion without MWCNTs. When the concentration of octadecanol

was 0.5 wt%, the supercooling decreased by 16.9 % and the thermal conductivity increased by 0.14 % and 0.05 %, respectively. When the concentration of octadecanol was 1.0 wt%, the supercooling decreased by 27. 1 % and the thermal conductivity decreased by 0.6 % and 1.1 %, respectively.

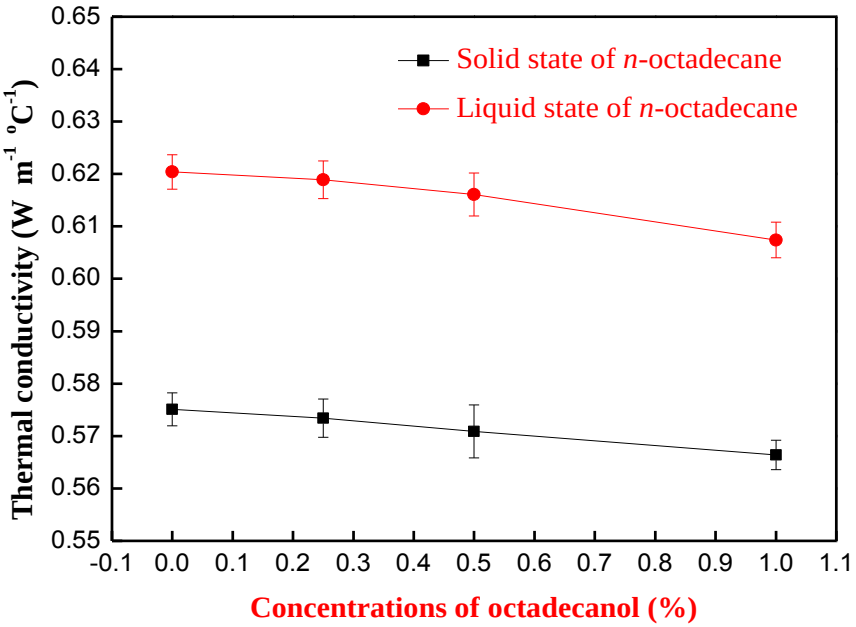

Fig.10. Thermal conductivity of 10 wt% NPCE with 0.1 wt% MWCNTs and various concentrations of octadecanol.

Figure 11 shows the thermal conductivity of 20 wt% *n*-octadecane emulsion containing 0.1 wt% MWCNT with various concentrations of octadecanol. The thermal conductivity of *n*-octadecane is 0.48 W/(m·K) at room temperature. The change of thermal conductivity of 10 wt% *n*-octadecane emulsion with various octadecanol concentrations was further verified by the change of thermal conductivity of 20 wt% *n*-octadecane emulsion with the increase in octadecanol concentration. Octadecanol reduces the thermal conductivity of nanoemulsion. When the concentration of octadecanol was 0.25 wt%, the supercooling decreased by 3.6 %, the thermal conductivity of nanoemulsion increased by 0.72 % (PCM at soild state) and 0.81 % (PCM at liquid state) compared

with 20 wt% *n*-octadecane nanoemulsion without MWCNTs, respectively. When the concentration of octadecanol is 0.5 wt%, the supercooling degree is reduced by 25.4 %, and the thermal conductivity is reduced by 0.23 % and 0.12 %, respectively. When the concentration of octadecanol was 1.0 wt%, the supercooling decreased by 36.4 % and the thermal conductivity decreased by 0.91 % and 0.84 %, respectively.

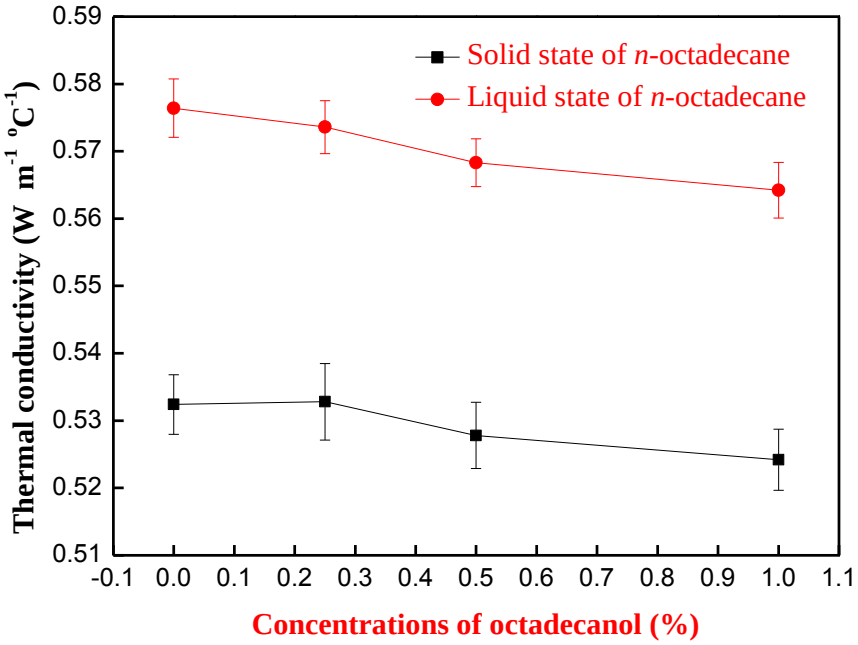

Fig.11. Thermal conductivity of 20 wt% NPCE with 0.1 wt% MWCNTs and various concentrations of octadecanol.

4. Conclusion

In this paper, a novel low supercooling and high thermal conductivity nano phase change emulsion with *n*-octadecane as PCM was successfully prepared, with MWCNTs utilised as high thermal conductivity material and octadecanol as nucleating agent. Dynamic light scattering analysis showed that the nano phase change emulsion prepared had excellent dispersion and stability. In addition, the following conclusions can be drawn from the analysis of its thermal properties:

(1) the thermal conductivity of nanoemulsion increased linearly after 10 wt% *n*-octadecane was added to MWCNTs and it had little effect on the enthalpy of phase transition. When the concentration of MWCNTs reached 1 wt%, the thermal conductivity of the emulsion reached the highest. The enhancement ratios of 0.5923 W/(m·K) (solid state of *n*-octadecane) and 0.6443 W/(m·K) (liquid state of *n*-octadecane) were 3.89 % and 4.32 %, respectively. The thermal conductivity of PCMs in liquid phase is higher than that in solid phase.

(2) When octadecanol was added into 10 wt% *n*-octadecane nanoemulsion containing 0.1 wt% MWCNTs, the supercooling degree of the emulsion gradually decreased with the increase in octadecanol concentration while the thermal conductivity and the enthalpy of phase transition decreased at the same time. When the octadecanol concentration was 1 wt%, the supercooling degree of emulsion decreased by 27.1 % from 16.6 ℃ to 12.1 ℃. When 1.0 wt% octadecanol was added to the 20 wt% emulsion containing 0.1 wt% MWCNTs, the supercooling decreased by 36.4 % from 17.3 ℃ to 11.0 ℃.

(3) When 10 wt% and 20 wt% *n*-octadecane nanoemulsion containing 0.1 wt% MWCNTs was added with 0.5 wt% octadecanol as nucleating agent, the thermal conductivity increased and the supercooling degree decreased. According to above findings, the PCM nanoemulsion prepared can be employed as the heat transfer and energy storage fluids for potential application in thermal systems.

Acknowledgement

This work was supported by National Natural Science Foundation of China (Nos.51976126, 51406121, 51876130), Shanghai Pujiang Program (No.18PJ1408900), Youth Eastern Scholar Program of Shanghai Municipal Education Commission, and Capacity Building Plan for some Non-military Universities and Colleges of Shanghai Scientific Committee (No. 18060502600).

References

1. Zhao, C.Y. and G.H. Zhang, *Review on microencapsulated phase change materials (MEPCMs): Fabrication, characterization and applications.* Renewable and Sustainable Energy Reviews, 2011. **15**(8): p. 3813-3832.
2. Dadollahi, M. and M. Mehrpooya, *Modeling and investigation of high temperature phase change materials (PCM) in different storage tank configurations.* Journal of Cleaner Production, 2017. **161**: p. 831-839.
3. Munyalo, J.M., X. Zhang, and X. Xu, *Experimental investigation on supercooling, thermal conductivity and stability of nanofluid based composite phase change material.* Journal of Energy Storage, 2018. **17**: p. 47-55.
4. Milián, Y.E., A. Gutiérrez, M. Grágeda, and S. Ushak, *A review on encapsulation techniques for inorganic phase change materials and the influence on their thermophysical properties.* Renewable & Sustainable Energy Reviews, 2017. **73**: p. 983-999.
5. Abhat, A., *Low temperature latent heat thermal energy storage: Heat storage materials.* Solar Energy, 1983. **30**(4): p. 313-332.
6. Zhang, P., Z.W. Ma, and R.Z. Wang, *An overview of phase change material slurries: MPCS and CHS.* Renewable and Sustainable Energy Reviews, 2010. **14**(2): p. 598-614.
7. Qiu, L., Y. Ouyang, Y. Feng, and X. Zhang, *Review on micro/nano phase change materials for solar thermal applications.* Renewable Energy, 2019. **140**: p. 513-538.
8. Wang, F., W. Lin, Z. Ling, and X. Fang, *A comprehensive review on phase change material emulsions: Fabrication, characteristics, and heat transfer performance.* Solar Energy Materials and Solar Cells, 2019. **191**: p. 218-234.
9. Alkan, C. and A. Sari, *Fatty acid/poly(methyl methacrylate) (PMMA) blends as form-stable phase change materials for latent heat thermal energy storage.* Solar Energy, 2008. **82**(2): p. 118-124.
10. Liu, Z., Z. Chen, and F. Yu, *Microencapsulated phase change material modified by graphene*

oxide with different degrees of oxidation for solar energy storage. Solar Energy Materials and Solar Cells, 2018. **174**: p. 453-459.

11. Alvarado, J.L., C. Marsh, C. Sohn, M. Vilceus, V. Hock, G. Phetteplace, and T. Newell, *Characterization of supercooling suppression of microencapsulated phase change material by using DSC.* Journal of Thermal Analysis & Calorimetry, 2006. **86**(2): p. 505-509.
12. Zhu, K.Y., W. Shuang, Q.I. Heng-Zhi, L.I. Hui, Y.H. Zhao, and X.Y. Yuan, *Supercooling Suppression of Microencapsulated n-Alkanes by Introducing an Organic Gelator.* Chemical Research in Chinese Universities, 2012. **28**(3): p. 539-541.
13. Al-Shannaq, R., J. Kurdi, S. Al-Muhtaseb, M. Dickinson, and M. Farid, *Supercooling elimination of phase change materials (PCMs) microcapsules.* Energy, 2015. **87**: p. 654-662.
14. Sarı, A., C. Alkan, D.K. Döğüşcü, and Ç. Kızıl, *Micro/nano encapsulated n-tetracosane and n-octadecane eutectic mixture with polystyrene shell for low-temperature latent heat thermal energy storage applications.* Solar Energy, 2015. **115**: p. 195-203.
15. Wang, H., J. Luo, Y. Yang, L. Zhao, G. Song, and G. Tang, *Fabrication and characterization of microcapsulated phase change materials with an additional function of thermochromic performance.* Solar Energy, 2016. **139**: p. 591-598.
16. Yang, R., H. Xu, and Y. Zhang, *Preparation, physical property and thermal physical property of phase change microcapsule slurry and phase change emulsion.* Solar Energy Materials and Solar Cells, 2003. **80**(4): p. 405-416.
17. Mo, S.P., Y. Chen, J.Y. Yang, and X.L. Luo, *Experimental Study on Solidification Behavior of Carbon Nanotube Nanofluid.* Advanced Materials Research, 2011. **171-172**: p. 333-336.
18. Liu, Y., J. Wang, C. Su, S. Geng, Y. Gao, and Q. Peng, *Nucleation rate and supercooling degree of water-based graphene oxide nanofluids*. Applied Thermal Engineering, 2016. **115**.
19. Huang, L., E. Günther, C. Doetsch, and H. Mehling, *Subcooling in PCM emulsions—Part 1: Experimental.* Thermochimica Acta, 2010. **509**(1): p. 93-99.

20. Shao, J., J. Darkwa, and G. Kokogiannakis, *Review of phase change emulsions (PCMEs) and their applications in HVAC systems.* Energy and Buildings, 2015. **94**: p. 200-217.
21. Wang, F., C. Zhang, J. Liu, X. Fang, and Z. Zhang, *Highly stable graphite nanoparticle-dispersed phase change emulsions with little supercooling and high thermal conductivity for cold energy storage.* Applied Energy, 2017. **188**: p. 97-106.
22. Zhang, S., J.Y. Wu, C.T. Tse, and J. Niu, *Effective dispersion of multi-wall carbon nano-tubes in hexadecane through physiochemical modification and decrease of supercooling.* Solar Energy Materials & Solar Cells, 2012. **96**(1): p. 124-130.
23. Shao, J., J. Darkwa, and G. Kokogiannakis, *Development of a novel phase change material emulsion for cooling systems.* Renewable Energy, 2016. **87**: p. 509-516.
24. Zhang, X., J. Niu, S. Zhang, and J.Y. Wu, *PCM in Water Emulsions: Supercooling Reduction Effects of Nano□Additives, Viscosity Effects of Surfactants and Stability.* Advanced Engineering Materials, 2015. **17**(2): p. 181-188.
25. Wang, F., J. Liu, X. Fang, and Z. Zhang, *Graphite nanoparticles-dispersed paraffin/water emulsion with enhanced thermal-physical property and photo-thermal performance.* Solar Energy Materials & Solar Cells, 2016. **147**: p. 101-107.
26. Puupponen, S., A. Seppälä, O. Vartia, K. Saari, and T. Ala-Nissilä, *Preparation of paraffin and fatty acid phase changing nanoemulsions for heat transfer.* Thermochimica Acta, 2015. **601**: p. 33-38.
27. Zhang, Z., Y. Yuan, N. Zhang, and X. Cao, *Experimental investigation on thermophysical properties of capric acid–lauric acid phase change slurries for thermal storage system.* Energy, 2015. **90**: p. 359-368.
28. Wang, Y., S. Li, T. Zhang, D. Zhang, and H. Ji, *Supercooling suppression and thermal behavior improvement of erythritol as phase change material for thermal energy storage.* Solar Energy Materials & Solar Cells, 2017. **171**: p. 60-71.

29. Zalba, B., J.M.a. Marín, L.F. Cabeza, and H. Mehling, *Review on thermal energy storage with phase change: materials, heat transfer analysis and applications.* Applied Thermal Engineering, 2003. **23**(3): p. 251-283.

30. Chen, S.L., P.P. Wang, and T.S. Lee, *An experimental investigation of nucleation probability of supercooled water inside cylindrical capsules.* Experimental Thermal & Fluid Science, 1998. **18**(4): p. 299-306.

31. Zhang, G.H. and C.Y. Zhao, *Synthesis and characterization of a narrow size distribution nano phase change material emulsion for thermal energy storage.* Solar Energy, 2017. **147**: p. 406-413.

32. Zhang, G.H., S.A.F. Bon, and C.Y. Zhao, *Synthesis, characterization and thermal properties of novel nanoencapsulated phase change materials for thermal energy storage.* Solar Energy, 2012. **86**(5): p. 1149-1154.

33. Marconnet, A.M., M.A. Panzer, and K.E. Goodson, *Thermal conduction phenomena in carbon nanotubes and related nanostructured materials.* Reviews of Modern Physics, 2013. **85**(3): p. 1295-1326.

34. Asua, J.M., *Miniemulsion polymerization.* Progress in Polymer Science, 2002. **27**(7): p. 1283-1346.

35. Black, J.K., L.E. Tracy, C.P. Roche, P.J. Henry, J.B. Pesavento, and T. Adalsteinsson, *Phase Transitions of Hexadecane in Poly(alkyl methacrylate) Core−Shell Microcapsules.* The Journal of Physical Chemistry B, 2010. **114**(12): p. 4130-4137.

36. Günther, E., L. Huang, H. Mehling, and C. Dötsch, *Subcooling in PCM emulsions – Part 2: Interpretation in terms of nucleation theory.* Thermochimica Acta, 2011. **522**(1): p. 199-204.

37. Garg, P., J.L. Alvarado, C. Marsh, T.A. Carlson, D.A. Kessler, and K. Annamalai, *An experimental study on the effect of ultrasonication on viscosity and heat transfer performance of multi-wall carbon nanotube-based aqueous nanofluids.* International Journal of Heat and

Mass Transfer, 2009. **52**(21): p. 5090-5101.

38. Babaei, H., P. Keblinski, and J.M. Khodadadi, *Thermal conductivity enhancement of paraffins by increasing the alignment of molecules through adding CNT/graphene.* International Journal of Heat and Mass Transfer, 2013. **58**(1): p. 209-216.

39. Xue, L., P. Keblinski, S.R. Phillpot, S.U.S. Choi, and J.A. Eastman, *Effect of liquid layering at the liquid–solid interface on thermal transport.* International Journal of Heat and Mass Transfer, 2004. **47**(19): p. 4277-4284.

40. Xue, Q.Z., *Model for the effective thermal conductivity of carbon nanotube composites.* Nanotechnology, 2006. **17**(6): p. 1655.